Geomorphology 125 (2011) 421–432

Contents lists available at ScienceDirect

Geomorphology

journal homepage: www.elsevier.com/locate/geomorph

Sediment transfer patterns at the Illgraben catchment, Switzerland: Implications for the time scales of debris flow activities

Catherine Berger [a,b,*], Brian W. McArdell [a], Fritz Schlunegger [b]

[a] Swiss Federal Research Institute WSL, Zürcherstrasse 111, CH-8903 Birmensdorf, Switzerland
[b] Institute of Geological Sciences, University of Bern, Baltzerstrasse 1+3, CH-3012 Bern, Switzerland

ARTICLE INFO

Article history:
Received 30 April 2010
Received in revised form 7 October 2010
Accepted 8 October 2010
Available online 17 October 2010

Keywords:
Debris flows
Sediment transfer pattern
Erosion and deposition
Entrainment
Aerial images
Photogrammetry

ABSTRACT

Debris flows strongly control sediment transfer patterns in mountainous catchments. We quantify sediment transfer at the Illgraben, Switzerland, where debris flows are frequent and geomorphic change is rapid. Four sequential aerial image series (from fall 2007 to fall 2009) were used to measure landscape change in relation to debris flows. The debris, often originating from bedrock landslides, was transported in patterns of erosion, storage, and remobilization. The landslides typically stopped on the downslope hillslope or in the channel, and they did not transform directly into debris flows. The magnitude and nature of sediment transfer patterns show large spatial and temporal variability, and the storage time of the deposits was shorter than one year. Landslide volumes were an order of magnitude smaller than the debris flows at the catchment outlet. While the mechanism of debris flow initiation could not be determined unambiguously, clearly debris flows must entrain substantial amounts of sediment along the flow path to attain the volumes estimated at the distal end of the fan.

1. Introduction

Debris flows are an important process in landscape evolution (e.g., Stock and Dietrich, 2006) and pose significant hazards in mountain areas (e.g., Jakob and Hungr, 2005). Yet their spatial and temporal variability is poorly understood. Debris flow occurrence requires steep slopes and availability of debris and water (e.g., Major et al., 2005). The Illgraben catchment in the western Swiss Alps produces one to four debris flows every year, providing an opportunity to investigate the conditions that characterize debris flow activity (Schlunegger et al., 2009). In this paper we quantify landscape changes along with seasonal and annual patterns of sediment transport in the Illgraben catchment.

Initiation mechanisms of debris flows include the transformation of landslides into debris flows (e.g., Wieczorek, 1987; Iverson et al., 1997; Imaizumi and Sidle, 2007), entrainment and bulking of sediment transporting floods (and eventually the process transformation to debris flows) by water flow over loose sediment deposits at the toe of a cliff (e.g., Larsen et al., 2006; Coe et al., 2008), or in-channel mobilization and entrainment of debris by water runoff in a channel (e.g., Berti et al., 1999; Cannon and Reneau, 2000). Recently, air-photo based studies have reported the dominance of debris slides transforming into debris flows in unglaciated (e.g., Imaizumi and Sidle, 2007) and formerly glaciated settings (e.g., Brardinoni et al., 2009). Alternatively, debris flows can transform from an initially small flow to a large, hazardous event by entraining sediment from the channel bed and banks into the flow (Gallino and Pierson, 1984; Fannin and Rollerson, 1993; Jakob et al., 2005; Santi et al., 2008). The availability of debris along a transit path is therefore of critical importance for the formation of large debris flows. Cycles of channel scour and aggradation were described, e.g., by Benda (1990), Rickenmann and Zimmermann (1993), Bovis and Jakob (1999), Jakob et al. (2005), and Fuller and Marden (2010). This cut-and-fill pattern is crucial because temporal and spatial variation of debris availability is a key parameter in the prediction of debris flow activity (Zimmermann et al., 1997; Bovis and Jakob, 1999) with respect to the potential for the study channel to overcome intrinsic triggering thresholds: a recently scoured channel will have a lower probability of debris flow occurrence.

Sediment budgets together with information about the spatial and temporal variability of the transfer processes have been used to characterize catchments in terms of, e.g., geomorphic activity or seasonality (e.g., Jäckli, 1957; Dietrich and Dunne, 1978; Benda, 1990; Fuller and Marden, 2010). The linkages between transport processes and storage elements are important (e.g., Dietrich et al., 1982), as well as the role of storage elements (Schrott et al., 2003; Slaymaker et al., 2003).

Despite the abundance of studies addressing the origin, the mechanisms and the magnitudes of debris flows in mountainous settings as summarized previously, little is known about the time scales of sediment discharge of these flows on an annual and seasonal

* Corresponding author. Swiss Federal Research Institute WSL, Zürcherstrasse 111, CH-8903 Birmensdorf, Switzerland. Tel.: +41 44 739 24 42.
E-mail addresses: catherine.berger@wsl.ch (C. Berger), brian.mcardell@wsl.ch (B.W. McArdell), fritz.schlunegger@geo.unibe.ch (F. Schlunegger).

0169-555X/$ – see front matter © 2010 Elsevier B.V. All rights reserved.
doi:10.1016/j.geomorph.2010.10.019

basis. In particular, the variabilities of production, storage and transport of sediment in debris flow dominated catchments have not yet been explored in sufficient detail. In this study, we aim to quantify catchment-wide sediment dynamics over high temporal and spatial resolution in the active part of the Illgraben using sequential aerial image series that can document sediment dynamics at the annual and seasonal scales (i.e., fall 2007, summer 2008, fall 2008, and fall 2009). We used photogrammetric methods to measure topographic changes in the debris flow source area and compared the results with sediment discharge data from the end of the fan. Because the pattern of sediment transfer at the Illgraben can be described by sediment sinks and sources with erosion, deposition, and remobilization on a seasonal basis, we will use the comparison between sediment storage areas and debris flow volume in an effort to quantify

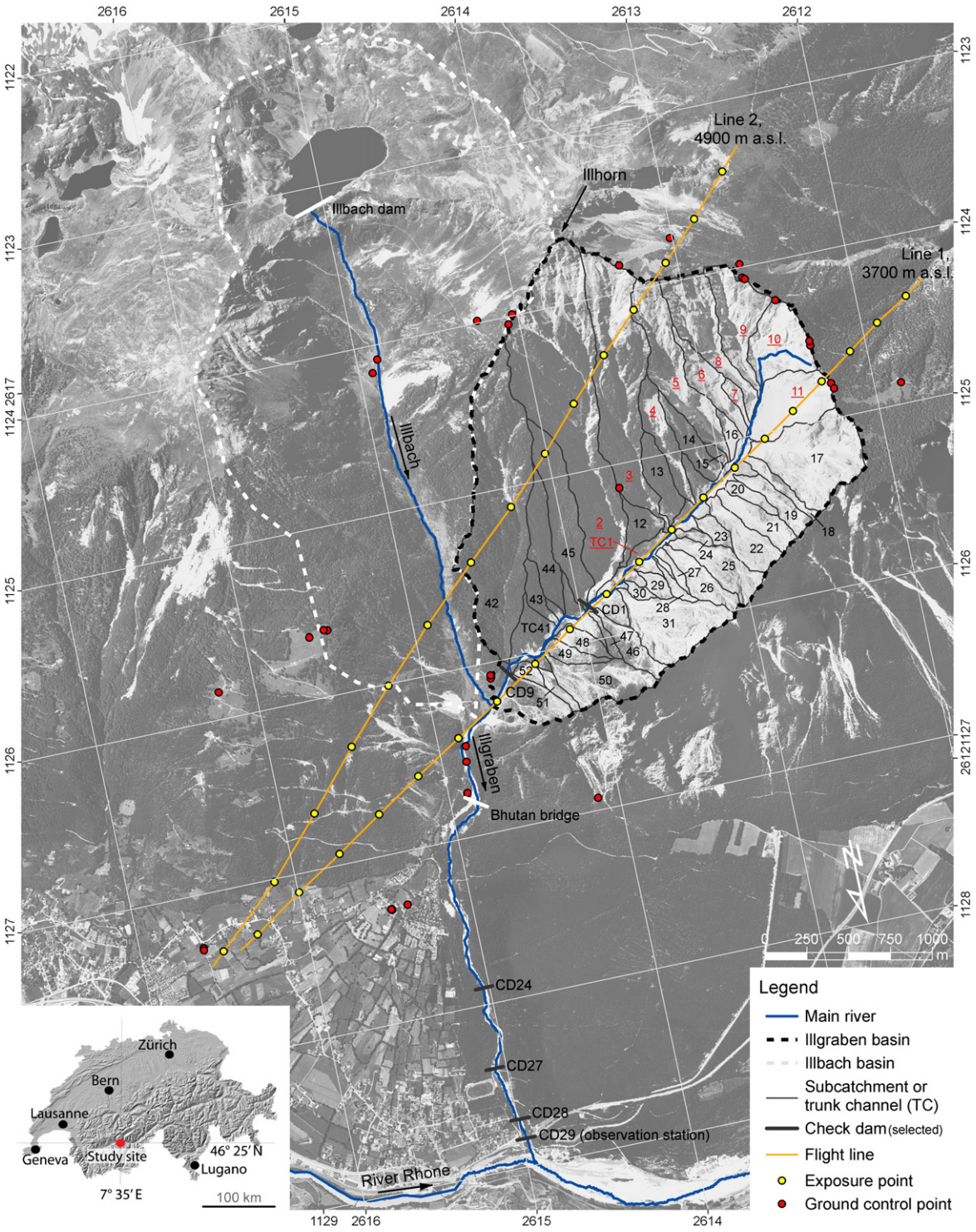

Fig. 1. Overview of the Illgraben catchment. The Illgraben and Illbach basin are displayed together with the main river network, the subcatchments (SC), and trunk channels (TC) of the Illgraben basin above check dam 9, the Illbach dam, selected check dams, and the Bhutan foot bridge. The flight lines of the image surveys are indicated, including the locations where an image was taken (exposure points), and ground control points are shown. Subcatchments labeled with red underlined numbers were investigated in detail. The orthophoto (swissimage© 2010) and relief of Switzerland are reproduced with authorization from swisstopo DV033594 (swissimage) and JA082265 (relief).

the importance of sediment entrainment in the formation of channelized debris flows.

2. Field site

The Illgraben in Switzerland (Fig. 1) is well known for the frequently observed sediment transport and debris-flow events that reach the basin outlet (see Badoux et al., 2009) with one to four debris flows observed, on average, every year. The 10.4 km^2-large northward-facing basin is located in the western part of Switzerland and extends from the summit of the Illhorn (2716 m asl), through a fan (apex at 850 m asl), and to the outlet of the Illgraben into the River Rhone (610 m asl). It consists of two tributary basins, the Illgraben catchment (4.7 km^2; Fig. 1), which experiences significant debris flow activity, and the Illbach tributary basin (5.7 km^2). The Illbach catchment is not considered in this study because the headwaters (upper 1.6 km^2) have been hydrologically isolated from the rest of the catchment by the construction of the Illsee dam (Fig. 1) in 1923, and therefore contributes little to the total Illgraben discharge. The channel of the Illbach is narrow and choked with vegetation, indicating that it does not convey much sediment. Additionally, the Illbach basin joins the Illgraben as a hanging valley, indicating that its rate of channel incision is much lower and little geomorphic evidence was found for debris flow activity.

The climate at the Illgraben is temperate-humid with a relatively low annual precipitation, influenced by the rain shadow effect within an intra-Alpine valley. Mean annual precipitation ranges from 700 mm in the lower part to 1700 mm in the summit region. Intense rainstorms occur mainly in summer (Hürlimann et al., 2003). The Illgraben catchment is underlain by Triassic metasedimentary rocks. A large anticline, offset by a fault, separates the limestones on the western flank from the highly fractured quartzites with interbedded dolomites and schists on the north face of the Illhorn. The trunk channel follows the SW–NE striking fault that dissects the axial plane of this anticline (Schlunegger et al., 2009). Forty-four percent of the Illgraben catchment is covered by bedrock and debris deposits, 42% is covered by forest and 14% by grassland (Badoux et al., 2009). The debris fan is unusually large for the Alps, with a radius of about 2 km. The fan volume is estimated at $500 \cdot 10^6$ m^3, with a slope angle of about 5.7° (Badoux et al., 2009).

The catchment is characterized by persistent rockfall, landsliding, debris avalanches, and debris flows. Annual sediment discharge over the past 10 years is estimated at about 100,000 m^3 of sediment by debris flows alone (McArdell and Graf, 2009). A large variety of flow types has been observed, spanning the range from granular debris flows to muddy debris flows, to hyperconcentrated flows and floods (Badoux et al., 2009). Debris flows typically occur during intense thunderstorms between May and October. A nearly 50 m-high debris retention dam referred to as check dam CD1 (Fig. 1) was built between 1967 and 1969 as a countermeasure after a large rock avalanche occurred in 1961 (estimated volume 3,500,000 m^3; Lichtenhahn, 1971; Gabus et al., 2008). The torrent channel downstream of CD1 was protected by 28 additional check dams, most of which are still present. These check dams help ensure that the channel on the fan is stabilized at a relatively low channel depth, resulting in a channelized streambed with a relatively large discharge capacity.

We divided the catchment above check dam CD9 (Fig. 1) into subcatchments (SC) with channel drainage areas >10,000 m^2 (Fig. 1); the trunk channel TC1 and the tributary channel TC41 are the channels above and below CD1, respectively. Subcatchments SC2–SC11 and SC42 are on the southeastern flank and are underlain by massive white quartzites, conglomeratic quartzites, and layers of schists. The total size and portion of active area within the subcatchments (nonvegetated and connected to the torrent; Schlunegger et al., 2009) varies greatly. Mean slopes are steep, increasing upstream from 36° close to CD1 to 42° in the rear part of the Illgraben in subcatchment SC11. The NW side of the catchment is composed of massive limestones and dolomites with steep slopes (mean slope 42° for subcatchments SC17–SC31). These rock faces are the sources for frequent rockfall, but have not produced debris flows (Schlunegger et al., 2009).

An automated observation station, in operation since 2000 (Rickenmann et al., 2001; Hürlimann et al., 2003), is located on the lower third of the debris fan. A horizontal force plate, installed on the channel bed at check dam CD29 (Fig. 1), records total normal and shear force (McArdell et al., 2007). The height of transient debris-flow surfaces, video, geophone measurements, and weather information are recorded at different places on the fan and in the catchment.

3. Methods

We used a variety of data and methods to quantify the sediment transfer patterns in the catchment. We analyzed aerial images with photogrammetric methods (Section 3.1), identified debris flow active subcatchments, constructed digital terrain models (DTMs), and mapped surface changes (Section 3.2). We used commercially available DTMs (DTM AV, year 2005 and DTM 25, year 1986 by swisstopo) to delineate and characterize the subcatchments (Section 3.3). Maximum elevation changes of the channel surface for the same intervals as for the aerial image surveys were determined at the Bhutan foot bridge (Fig. 1), at check dam CD27, and between CD28 and CD29 (Section 3.3) to compare downstream variation of topographic change in the channel. Data from the force plate at CD29 was used to calculate flow parameters and sediment export by debris flows at the Illgraben outlet (Section 3.4). The following sections describe each of these methods in detail.

3.1. Aerial surveys and image orientation

Sediment transfer observations and allocation of sediment sources within the upper catchment, the area where debris flows are considered to originate (above the check dam CD1 in Fig. 1; Schlunegger et al., 2009), were based on analysis of four aerial image series taken on 2 October 2007, 15 July 2008, 29 September 2008, and 23 September 2009. Land surface changes between image series were investigated for two seasonal intervals, “spring 2008” (2 October 2007–15 July 2008) and “summer 2008” (15 July–29 September 2008), and for two annual intervals “year 2008” (2 October 2007–29 September 2008) and “year 2009” (29 September 2008–23 September 2009). The selection of the time of image acquisition was guided by the snow cover, the weather conditions (i.e., clear sky), and was bracketed by the start and the end of the debris flow season. Accordingly, the images from 15 July 2008 correspond to the time when the ground surface was free of snow except for some snow accumulations at the core of the subcatchments SC8–SC11 (Fig. 1). The aerial surveys in fall 2007, 2008, and 2009 were taken before snowfall began and at the end of the debris-flow season. The durations of the survey periods thus differ in the lengths of the time intervals. Most important, however, the selected periods share the same pattern as they cover both winter and summer seasons and thus allow the quantification of sediment discharge on a seasonal basis.

The analogue air-survey camera (Leica RC30, 230 × 230 mm format used for the photogrammetry) has a nominal focal length of 300 mm. A total of 35 images, distributed on two image strips (Fig. 1), were taken with 80% longitudinal and 30–80% lateral overlap during each survey. Flight heights were adjusted to the elevations of the terrain. A lower strip at 3700 m asl follows the central axis of the Illgraben channel, and a second higher strip at about 4900 m asl covers the Illhorn flank. Consequently, the scale varies between 1:5000 and 1:9000. After the flights, the images were scanned at 15 μm (VEXCEL UltraScan5000; Gruber and Leberl, 2001), with a pixel size corresponding to 0.1–0.2 m on the ground. Further methodological

details regarding the aerotriangulation of the images, the measurements of the fixpoints (Fig. 1), the details about the photogrammetric camera, and the correlation with the local Swiss coordinate system LV95 and corresponding elevation system LHN95 are presented in Berger (2010).

3.2. Photogrammetric terrain analysis

We identified the geomorphically active area (no vegetation and connected to the torrent) in all subcatchments at a scale of 1:3000 using the orthophoto from the summer 2008 survey and defined active segments as areas with no vegetation cover and direct connectivity with the gully. Note that we considered those hillslopes as connected with the Illgraben debris flow channel on which eroded material is directly supplied to the trunk channel TC1 (for justification see Schlunegger et al., 2009). Assessments of topographic changes were carried out in four steps. First, the subcatchments above check dam CD1 (Fig. 1) showing zones of elevation change or obvious evidence of recent debris flows (primarily lateral deposits) were identified on the first three image series. In the subcatchments beneath CD1, field observations showed that only tributary catchment SC42 experienced debris flow activity, but photogrammetric mapping of debris flow traces was not possible because large parts of that channel were obstructed by trees. Tributary catchments SC17–SC31 were sites of rock fall and small rock avalanche events in the past, but were not areas where debris flows originated (Hürlimann et al., 2003). Accordingly, these subcatchments were not mapped and changes not measured. DTMs were generated with manual stereo measurements. We focused on the trunk channel reach TC1 (Fig. 1) because this has been the segment of the largest changes in channel depth and storage volume (Hürlimann et al., 2003; Schlunegger et al., 2009).

Second, we calculated for all four surveys DTMs that cover the entire area surrounding the trunk channel TC1. The points were distributed on a 2-m quadratic grid (14,280 points, about 5.52 ha), and the same point locations were used for all image series. Elevations were measured manually in stereo, and the net elevation changes were calculated by subtracting the DTMs of different time steps. For the difference models and using the rule for error propagation, standard deviation in z-direction is

$$\sigma_{Diff} = \sqrt{\sigma_{step\,1}^2 + \sigma_{step\,2}^2} \quad (1)$$

with $\sigma_{step\ 1}$ and $\sigma_{step\ 2}$ being the standard deviations in z-direction of the DTMs. Because the images of all time steps were triangulated in one bundle, the DTMs have identical standard deviations in z-direction ($\sigma = 0.28$ m), and $\sigma_{Diff} = 0.39$ m. Consequently, height differences ranging from −0.4 to 0.4 m were discarded in the analysis of the difference models and volume calculations. Note that the error estimates certainly influence the calculations of the magnitude of sediment discharge, but will not alter the general conclusion of a strong seasonality in sediment discharge.

Third, we mapped the changes in the geomorphically active subcatchments (SC2–SC11) for areas of erosion and deposition. We then analyzed in stereo the images of the different surveys but with the same display window, and identified changes by comparison of the terrain elevation and image information (e.g., erosion scars and talus deposits). Minimum elevation difference for the detection of changes was estimated qualitatively at about 0.5 m. We noted snow deposits, but did not determine their thicknesses and volumes because partial cover by debris impeded the precise delineation of these areas. In the Results section, only residual snow deposits are displayed in order to show which areas were covered by snow. These areas are therefore excluded from the analysis.

Fourth, we measured elevations in the mapped subcatchments where the changes were >1 m that largely correspond to the error estimates of the method (−0.4 to 0.4 m, see previous discussion). Maximum and mean elevation changes and the areas of the features were then used to estimate volumetric changes. Given the large errors associated with the photogrammetry, we decided it was not useful to make further error analyses and instead we focus on the minimum and maximum estimates. Estimates of thickness variations in the middle of erosional or depositional features are on the order of 30%. Volumes of these latter features and volume changes in trunk channel TC1 derived from the DTMs are labeled as “measured” volumes. In contrast, “estimated” volumes refer to those sites where a change was observed and mapped, but the thickness of the eroded or accumulated sediment lies within the detection limit for vertical changes (Table 2). As outlined previously, these limits comprise a lower ($h = 0.5$ m) and upper ($h = 1.0$ m) bound that correspond to the detection limit and to the threshold value of the method, respectively. The values of these lower and upper bounds are then used to assess the “estimated volumes”.

3.3. Topographic analysis of the subcatchments and additional measurements on the fan

We used two DTMs to identify subcatchments and determine slopes. Below 2080 m asl, elevation data from airborne LiDAR (Light Detection and Ranging) are available on a 2.5-m grid (DTM-AV from Swisstopo, 2005). For higher elevations, data from a 25-m grid (DTM-25 from Swisstopo, 1986) were re-sampled to a 2.5-m grid and merged with the LiDAR data. We calculated flow direction and flow accumulation (Spatial Analyst, Arc GIS Arc Map 9.2) to obtain a stream network. The merged DTM was used to calculate slopes for each cell

Table 1
Debris flows and transitional events of 2008 and 2009.

Date	Front velocity[a] ($m\,s^{-1}$)	Flow depth[b,c] (m)	Number of surges[b]	Wet bulk density, maximum[b] ($kg\,m^{-3}$)	Max. discharge[b] ($m^3\,s^{-1}$)	Event volume[b] (m^3)	Subcatchment of origin[d] (field documentation)
Debris flows							
16 June 2008	2.4	1.13	1	2100	17	7800	above CD1 (not SC2)
1 July 2008	5.3	2.35/2.06	2	2000	101	59,900	SC42 + above CD1 (not SC2)
31 August 2008	1.9	1.39	1	2600	18	8200	above CD1
28 July 2009	2.2	0.99/0.81	2	2500	23	13,500	above CD1 (not SC2)
9 August 2009	5.9	2.56/1.65	2	1800	127	45,500	SC42 + SC2
Transitional events							
19 August 2008	N.D.[e]	0.5	1	1700	1	N.D.	N.D.
17 July 2009	N.D.	0.72	1	2000	3	N.D.	N.D.

[a] Front velocity determined from the travel time of the debris flow front between CD24 and CD29 using geophone signals.
[b] Values determined at the observation station at CD29.
[c] Flow depth is given for both surges (fist/s) when two surges were observed.
[d] Abbreviations stand for check dam (CD) and subcatchment (SC).
[e] N.D. = not determined.

and to construct orthophotos from the aerial surveys in fall 2007 and summer and fall 2008.

The Bhutan foot bridge crosses the Illgraben at about 845 m asl and is located beneath the fan apex (Fig. 1). We made digital terrain models of the channel underneath the bridge from close-range photogrammetry surveys after large torrential events and at the beginning and end of a debris flow season (usually May and October). Fixpoints were marked on the ground surface and surveyed with a total positioning instrument. Triangulation of the images resulted at a root mean squared error (RMSE) of 0.38 pixel in image space and of 0.005–0.01 (x- and y-direction) and 0.01 m (z-direction) in object space. The DTMs were matched automatically on a 0.05-m grid. Further details regarding the photogrammetric surveys including the calibration of the fix points are presented by Berger (2010).

Bed aggradation and erosion at the base of check dam 27 was derived from photographs taken after debris flow and flood events using the check dam crest and painted markings as a scale. No obvious scour holes were visible at the base of the check dam. We performed terrestrial surveys between check dams CD28 and CD29 (Fig. 1) with a total positioning instrument (Leica TC407). We sampled surface points manually. Additionally, terrace borders in the channel were used for optimal representation of the terrain.

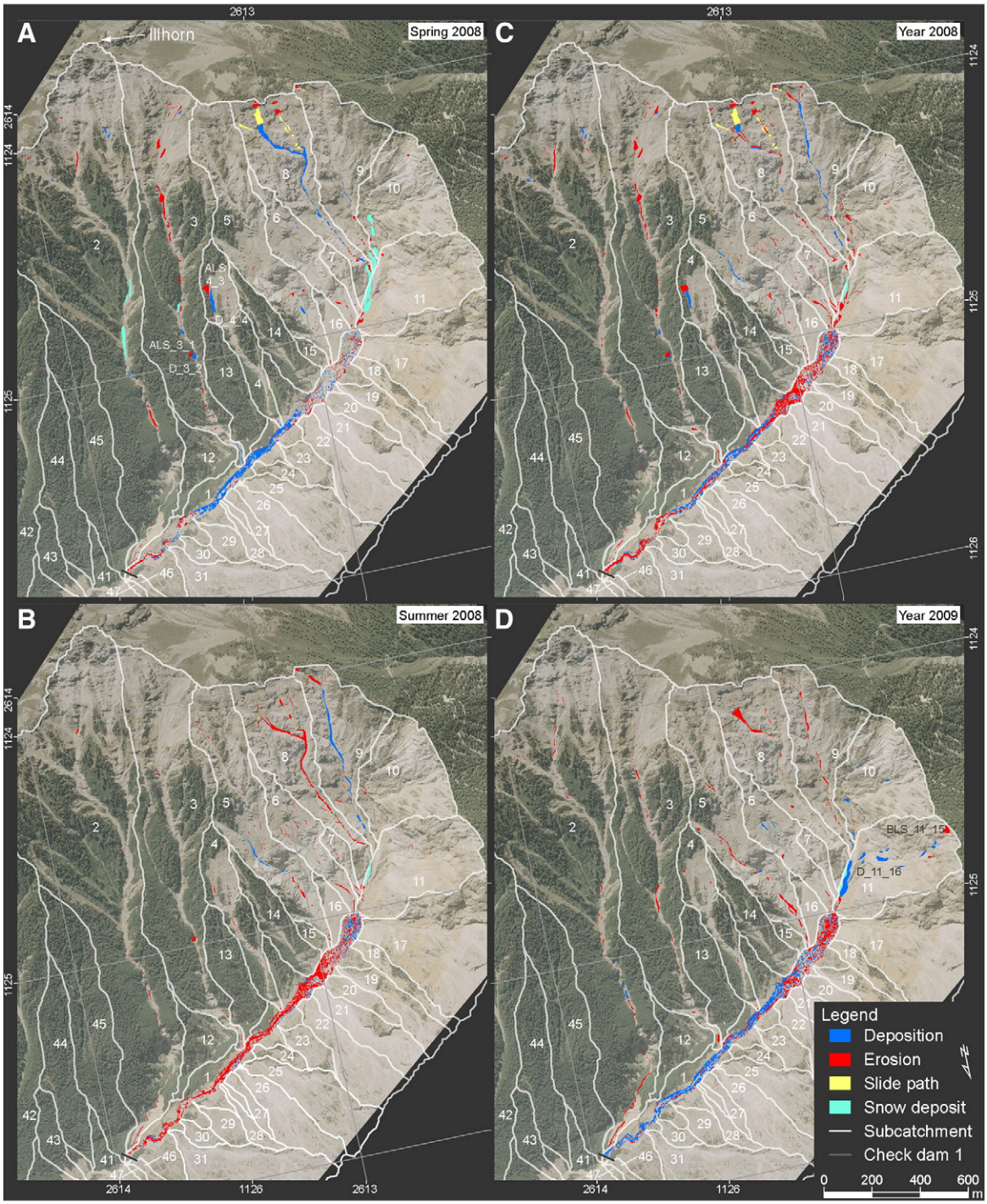

Fig. 2. Overview of the topographic change from 2007 to 2009 in the mapped subcatchments. (A) Spring 2008, (B) summer 2008, (C) year 2008, and (D) year 2009. Subcatchments are numbered; selected alluvial landslides (ALS), bedrock landslides (BLS) and deposits (D) are indicated; and their areas and volumes are given in Table 1. The orthophoto from Summer 2008 is displayed in the background.

3.4. Characterization of events

We analyzed the debris flows and transitional events with measurements from the observation station described by Hürlimann et al. (2003) and McArdell et al. (2007). The observation station is switched on automatically by ground vibrations when debris flows pass the geophone at check dam CD24 (Fig. 1). When active, data are recorded at 1 Hz. In the background-sampling mode, data are stored at a rate of one sample per 10 min, with mean, maximum, and minimum values, and the last instantaneous value. We used high resolution data for characterizing debris flows, and only considered maximum values from the background sampling mode for transitional events. Debris flows were characterized by a clearly visible front with a large number of boulders and tapering, muddy tail. Transitional events were represented by low density debris flows that displayed flash-flood-like fronts. During these flows, geophone impulse frequencies (defined as the frequency with which the geophone signal exceeds a small empirically determined positive voltage threshold value) were below the activation threshold of the observation station (see Badoux et al., 2009).

Flow depths h were recorded using laser and radar devices mounted on the bridge above the force plate at check dam CD29

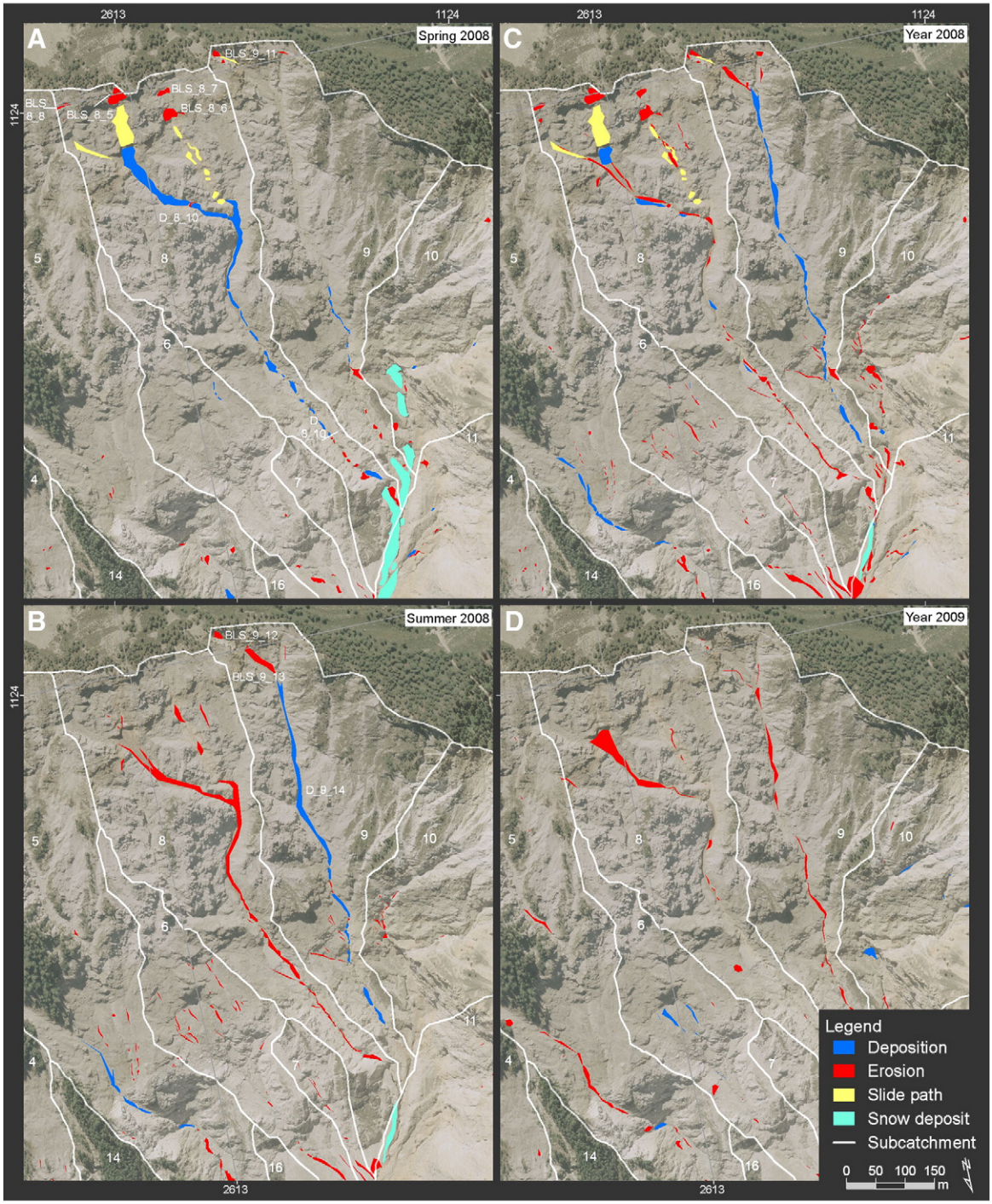

Fig. 3. Detail view of the topographic change from 2007 to 2009 for selected subcatchments. (A) Spring 2008, (B) summer 2008, (C) year 2008, and (D) year 2009. Subcatchments are numbered, selected bedrock landslides (BLS) and deposits (D) are indicated, and their areas and volumes are given in Table 2. The orthophoto from summer 2008 is displayed in the background.

(Fig. 1). During debris flows, we used laser data because the laser responds more quickly to rapid height fluctuations than the radar, as recognized by experience during the past years. We used radar data during the other events because radar more reliably records the turbulent water surface elevation. Total normal force F_N and shear force F_H were measured at the force plate (see McArdell et al., 2007). We calculated wet bulk density ρ of the flowing mixture, assumed lithostatic pressure for the mixture (no vertical acceleration) and used the ratio of normal stress σ to flow depth h, $\rho = \sigma/(g \cdot h)$, where g is the gravitational acceleration. All tare and initial values for flow height, shear, and normal force were taken from calibration periods at the force plate when no discharge was observed, and when the force plate was clean of sediment.

We calculated debris flow discharge as the product of front velocity and cross-sectional area at the force plate (Schlunegger et al., 2009). We estimated debris flow volume by integrating the discharge during the event and using the Strickler-equation to determine the flow velocity v_s (m s^{-1}):

$$v_s = k_s \cdot R^{2/3} \cdot S^{1/2} \quad (2)$$

where k_s is the roughness coefficient (back-calculated from the velocity of the front position of the flow; see Schlunegger et al., 2009 for more details), R is the hydraulic radius of the flow (m), and S is the upstream slope of the bed.

Transferred sediment volumes and denudation rates for the entire catchment were estimated from volumes and masses of the debris flows passing the observation station. For denudation rates, we calculated bedrock volume V_{br} by

$$V_{br} = \frac{V_{df} \cdot (\rho_{df} - \rho_{water})}{\rho_{br} - \rho_{water}} \quad (3)$$

where ρ is bulk density, V is volume, and subscripts $_{br}$ and $_{df}$ are for bedrock and debris flow, respectively. Bedrock bulk density ρ_{br} was set at 2650 kg m^{-3}, ρ_{water} at 1000 kg m^{-3}, and ρ_{df} was the mean wet bulk density of the debris flow estimated from measurements at the force plate.

4. Results

4.1. Seasonal change spring 2008

Between 2 October 2007 and 15 July 2008, two debris flows occurred (Table 1). The first debris flow was detected on 16 June (volume at the Illgraben outlet estimated at 9700 m^3), the second followed on 1 July (volume about 60,000 m^3). Field observations indicate that both events originated upstream of the confluence of tributary catchment SC2 and the trunk system. The lack of debris flow activity in SC2 was confirmed by inspection of the aerial images from summer 2008, which also showed no obvious change in the channel near the outlet of subcatchment SC2. However, we detected erosion in the upper and middle parts of the channel in SC2 (Fig. 2). Fresh debris flow traces were visible in the field in SC42 after the 1 July event, but we could not map the changes because large parts of the channel were obstructed by trees (Section 3.2).

The largest changes (Figs. 2 and 3; Table 2) were found in tributary catchments SC8 and SC9, where bedrock landslides (BLS) occurred at the catchment crest, and slide paths (SP) with a grooved surface and lighter color than the surrounding rock faces were visible. The total volume of the bedrock landslides and volume of eroded sediment along the slide path in SC8 was estimated at 5300 m^3 (Table 2). Most of the mobilized sediment was deposited and stored within the gully, and the total deposit volume estimated at about 5000 m^3 (D_8_10; Table 2 and Fig. 2). In subcatchment SC9, the bedrock landslide had an initial volume of about 500 m^3 (BLS_9_11), and some of the sediment was deposited in the lower part of the gully. In both SC8 and SC9, we found patches of erosion in the lower reaches.

Table 2
Properties of large landslides or erosion features and the related deposits.

Erosion			Deposition		
Label[a] and interval	Area (m^2)	Volume (m^3)	Label[a] and interval	Area (m^2)	Volume (m^3)
Spring 2008					
ALS_3_1	215	700	D_3_2	350	600
ALS_4_3	700	2100	D_4_4	1040	2100
BLS_8_5	490	2100	D_8_10	4820	5000
BLS_8_6	390	1100			
BLS_8_7	170	500			
BLS_8_8	90	300			
SP_8_9	2740	1300			
BLS_9_11	100	500			
Summer 2008					
BLS_9_12	130	500	D_9_14	2450	1200
BLS_9_13	585	900			
Year 2008					
TC1	20,200	11,700	TC1	11,400	9000
E_{est}	13,950	7000 to 13,900	D_{est}	6200	1900 to 3800
Year 2009					
BLS_11_15	630	4400	D_11_16	4800	3000
TC1	11,600	8500	TC1	19,800	12,200
E_{est}	11,600	5800 to 11,600	D_{est}	1600	800 to 1600

[a] Landslides and deposits are labeled according to a simple classification scheme (ALS: alluvial landslide, BLS: bedrock landslide, SP: slide path, D: deposit), subcatchment (SC) number and feature number (type_SC_#). Numbering of the features is chronological from the intervals and starts in the lowest-number SC with erosional features, continues with deposition in the same SC, and procedes similarly with the next SC. TC1 refers to trunk channel 1. E_{est} and D_{est} are estimates for mapped areas with erosion and deposition but without measurements for elevation change. Estimates are given for the lower ($h = 0.5$ m) and upper ($h = 1.0$ m) bounds based on photogrammetric estimation errors.

A landslide originating from a talus slope deposit (ALS_4_3; Fig. 2), with deposition of the mobilized mass after about 70 m displacement, occurred in subcatchment SC4; both the landslide and deposit (D_4_4) volumes were about 2100 m^3 (Table 2). We detected another landslide originating from a talus slope deposit (ALS_3_1; $V = 700$ m^3) in the lower part of SC3, and ca. 600 m^3 of sediment (D_3_2) was deposited about 20 m farther downslope. The changes in the remaining subcatchments above SC1 were small compared to these landslides (Figs. 2 and 4). Snow deposits from winter avalanches (more than 10 m thick) at the core of the subcatchment SC8–SC11 were visible on the aerial photographs of early summer 2008 (Figs. 2 and 3).

We divided the trunk channel TC1 (Figs. 5 and 6) into three zones based on the pattern of the changes in spring 2008: zone 1, the upstream reach with a channel bed surface of 27,200 m^2; zone 2, the middle reach with 18,300 m^2; zone 3, the downstream reach with 9700 m^2. Zone 2 showed accumulation across the entire channel, with up to 5-m thick deposits and a volume of 12,750 m^3. Sediment deposits in zone 3 were mostly eroded (up to 2 m elevation change close to check dam CD1), but sections with deposition and lateral deposits at channel bends were found as well. No clear pattern was visible in zone 1. Total volume changes for the entire trunk channel were 13,700 m^3 of deposition and 1900 m^3 of erosion.

In summary, photos covering the spring interval document several landslides with subsequent storage of the mobilized mass within the gullies. Trunk channel TC1 functioned as a sediment reservoir for the sediment from upstream catchments.

4.2. Seasonal change summer 2008

In summer 2008, a debris flow with a volume of 8200 m^3 occurred on 31 August, and a transitional event with a watery front was recorded on 19 August at the observation station (Table 1). The debris flow originated from above check dam CD1 (confirmed by field observations).

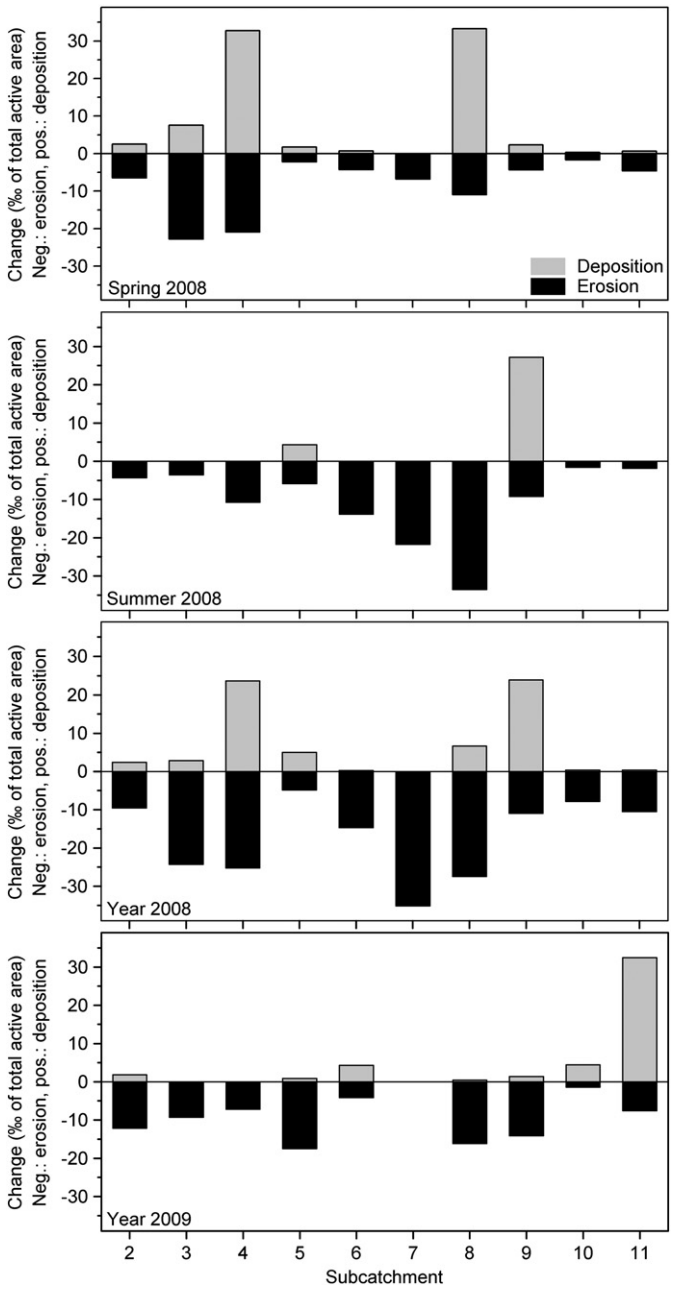

Fig. 4. Comparison of the change within each mapped subcatchment from 2007 to 2009. The change is displayed in per mil of the total active area (no vegetation and connected to the torrent considering all subcatchments) of a subcatchment; and is negative for erosion and positive for deposition.

Gully erosion mapped on aerial images of the lower part of the channel shows clear evidence of change in subcatchment SC2 (Fig. 2).

We found new bedrock landslides with estimated volumes of 500 m^3 (bedrock landslides BLS_9_12) and 900 m^3 (BLS_9_13) at the crest of tributary catchments SC9 (Fig. 3; Table 2), and the sediment was partly redeposited within the channel (about 1200 m^3, D_9_14). The deposits formed in the previous season (landslide deposits in tributary catchments SC8 and SC3) were largely eroded (Figs. 2 and 3). Patches of erosion and deposition were observed, e.g., in SC5; and about 30-m-long and 2-m-wide erosion scars were found on the talus deposits of SC6.

The trunk channel TC1 was scoured nearly along the entire length (Fig. 5). Maximum erosion was estimated at about 5 m, and the eroded debris had a volume of 13,700 m^3 for the entire reach. New levees were detected on the outside of the channel bends in zone 3. Total deposition in TC1 was 1350 m^3.

In the analyzed subcatchments (except SC5 and SC9), previously deposited debris was remobilized in the second half of the year, and erosion was the dominant process (Figs. 4 and 6). In contrast to the previous season when the trunk channel trapped sediment, the reach (e.g., trunk channel TC1, but also likely reaches farther downstream) was a source of sediment in summer 2008.

4.3. Annual change 2008

In the first year of the observations, between 2 October 2007 and 29 September 2008, sediment transported to the outlet by the debris flows had an estimated volume of about 80,000 m^3 (Table 1). Patterns of cycles of mobilization, storage, and remobilization (e.g., in SC8 on a seasonal basis) were much less apparent when observed over one year (Figs. 2 and 3). Therefore, erosion dominated in the mapped subcatchments (Fig. 4). The larger deposits visible on an annual basis are from the landslide in SC4 and from accumulations formed in the second half of the year in SC9.

The mass balance of trunk channel TC1 was negative, with 11,700 m^3 erosion and 9000 m^3 deposition (Fig. 6; Table 2). Zones 1 and 3 were sources of debris, and some small lateral deposits formed in zone 3 (Fig. 5). In zone 2, channel filling and subsequent scouring could only be observed in the seasonal analyses and were visible on an annual basis as lateral deposition (from the first interval) and thalweg erosion (from the second interval).

4.4. Annual change 2009

In the second year, from 29 September 2008 to 23 September 2009, two debris flows and one transitional event (17 July 2009) were registered. The debris flows occurred on 28 July and 9 August, with estimated volumes at the Illgraben outlet of 13,500 m^3 and 45,000 m^3, respectively (Table 1).

The 17 July debris flow originated from above the confluence of subcatchment SC2 and the trunk channel. Subcatchments SC2 and SC42 were active only during the 9 August debris flow, as revealed by field observations. The image analysis confirmed the activity of SC2, with some deposition in the channel and clear erosion of the gully in the lower part of the subcatchment (Fig. 2). Post-event field observations did not give a clear picture about debris flow occurrence in the upper catchment (above SC2) because the changes were small.

As in the preceding year, previously deposited sediment was remobilized in subcatchments SC8 and SC9 (Figs. 2 and 3). A bedrock landslide (BLS_11_15, volume estimated at 4400 m^3; Table 2) with subsequent downslope in-channel deposition occurred in SC11. The deposited volume was estimated at about 3000 m^3 (D_11_16). Linear gully erosion features were dominant in the remaining subcatchments (Fig. 4).

In the trunk channel TC1, the pattern of changes was similar to the previous annual interval (2008). Reaches with evidence for erosion along the thalweg and deposition on the lateral flanks of the Illgraben channel were found in zones 1 and 2 (Figs. 5 and 6). In contrast to the first year, zone 3 accumulated sediment, and lateral deposits were observed in the same areas where thalweg erosion was observed. The pattern with lateral deposition and central thalweg erosion suggests that the channel was first filled and subsequently emptied by erosion, similar to what we observed for the year before. The mass balance of TC1 showed net accumulation, with 12,200 m^3 of deposition and 8500 m^3 of erosion (Table 2).

4.5. Amplitude of geomorphic change in the catchment and on the fan

To gain a more general understanding of the changes in the entire Illgraben area, we sampled magnitudes of maximum erosion and

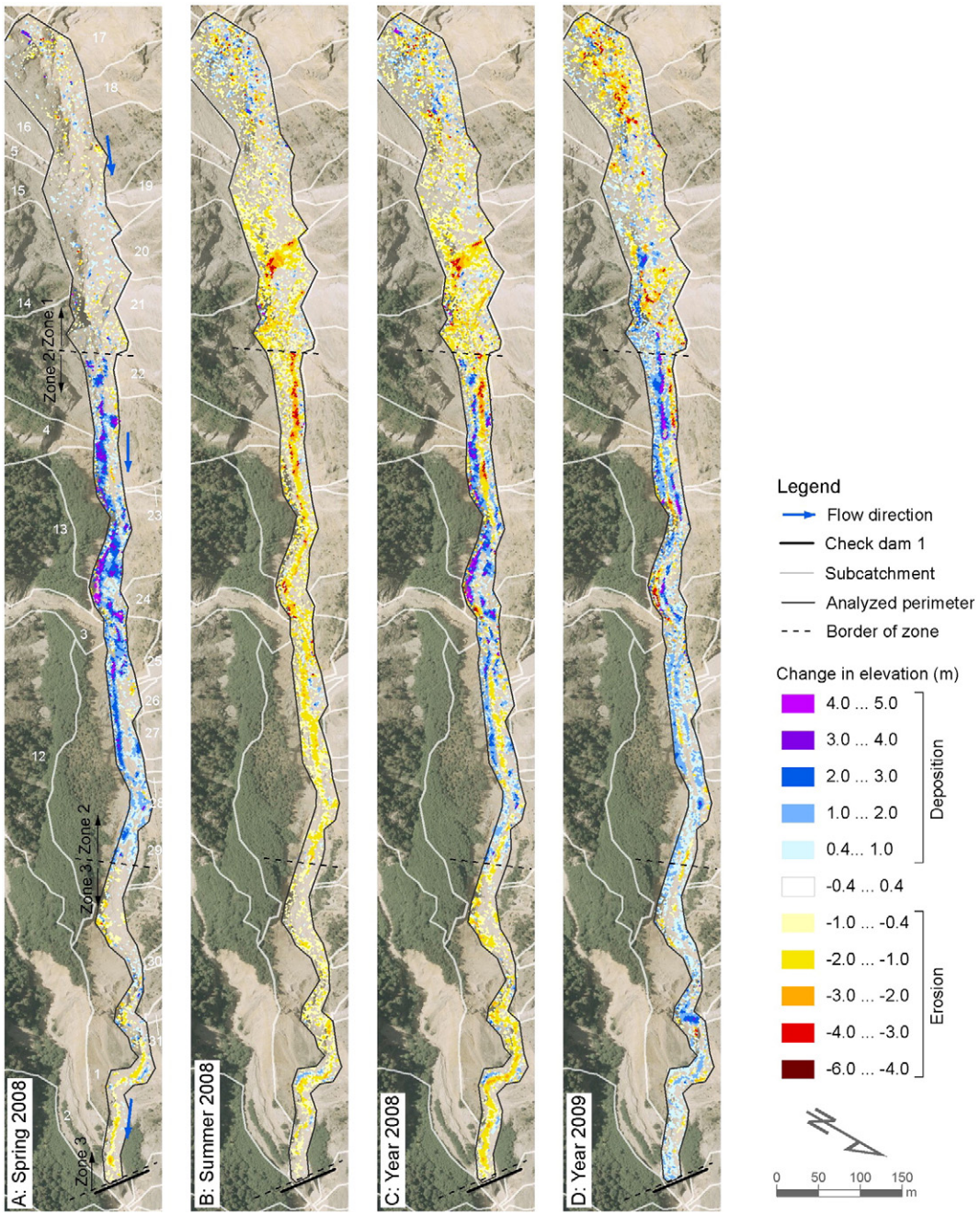

Fig. 5. Elevation change in trunk channel 1 from 2007 to 2009. (A) Spring 2008, (B) summer 2008, (C) year 2008, and (D) year 2009. The analyzed perimeter of the trunk channel (continuous black line) was divided into three zones (dashed lines), and elevation changes from −0.4 to 0.4 m are not colored. The elevation changes were calculated by subtraction of DTMs of different surveys, and grid size of the DTMs was 2 m. The orthophoto from Summer 2008 is displayed in the background.

deposition at different locations along the thalweg from the catchment crest to the outlet of the Illgraben into the River Rhone (Fig. 7). We observed both erosion and deposition along the profile and also in the channelized reaches beneath check dam CD1. The magnitude of maximum erosion is generally larger than that of maximum deposition. However, the magnitude of the changes decreased toward the outlet of the Illgraben. Similar downstream-decreasing amplitudes of sediment flux and storage were described by e.g., Benda and Dunne (1997a).

5. Discussion

5.1. Sediment transfer patterns

Sediment transfer patterns show a large spatial and temporal variability in the analyzed subcatchments (Figs. 2 and 3). The storage time of landslide deposits in the steep subcatchments and sediment deposits along the trunk channel appears to be <1 year. Therefore, most deposits are only visible in the seasonal analyses and are not preserved on an annual basis. In addition, net erosion is dominant in the upper catchment (Fig. 4). In the study period, trunk channel TC1 operated as a large sediment reservoir that was aggrading in the first half of the year between winter and spring, and degrading in the second half between summer and autumn. On an annual basis, this sequence changed to a pattern of lateral deposition during the first half of the year, and thalweg erosion between summer and autumn. Note that because of the time intervals between the surveys (2 to 12 months) and the occurrence of various seasonally based hydro-geomorphic processes that have modified the catchment topography (e.g., debris flows, floods, avalanches, and rockfall), the inferred seasonal effects are lumped and mainly based on the observed net

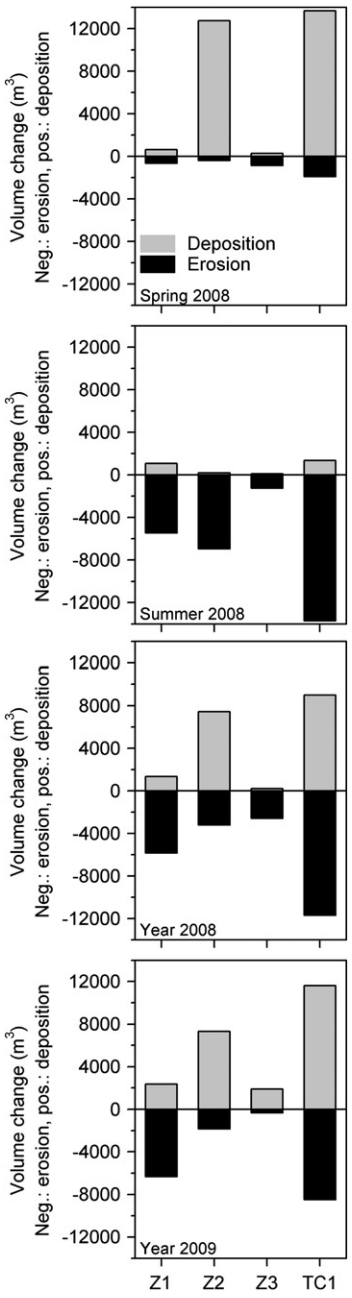

Fig. 6. Volume change in trunk channel 1 from 2007 to 2009 for each zone (z) and for the entire reach (TC1). The analyzed perimeter and the three zones are displayed in Fig. 5. Change is negative for erosion and positive for deposition and was calculated by subtraction of DTMs of different time steps.

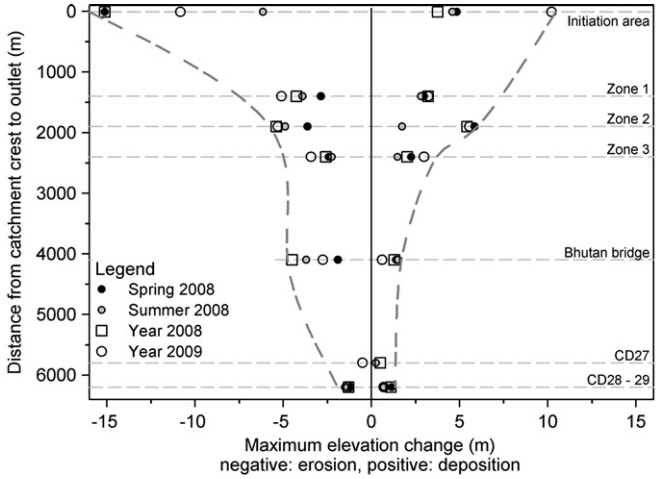

Fig. 7. Horizontal distance from the catchment crest versus maximum elevation change (both erosion and deposition) for each aerial image interval. Elevation change is negative for erosion and positive for deposition and was determined at different locations along the thalweg (Fig. 1). An envelope is given for the largest changes. Deposition in all cases was in gullies ("initiation area") or in channels, whereas erosion was estimated from a landslide ("initiation area") or in channels.

changes. Cycles of erosion and deposition within the observed sequences cannot be detected at a higher resolution. To address these problems, surveys would have to be performed after every significant debris flow event.

The observed sediment influx to the channel network occurs as a complex series of pulses, similar to the pattern described by Benda and Dunne's (1997b) stochastic model. Downslope sequences of sediment production, deposition, and re-erosion were previously found in semiarid, snowmelt-dominated networks by Schumm (1977) and more recently by Fuller and Marden (2010) in New Zealand, where sediment supply from gullies was seasonally variable, and mass movements contributed large quantities of sediment to the channels. Here, we illustrate quantitatively the seasonality of sediment dynamics in a steep headwater basin in the central European Alps. In this context, lithological observations of cobbles and boulders at three sites distributed over the Illgraben fan (Schlunegger et al., 2009) showed similar proportions of the different lithologies present in the catchment, indicating that sediment deposited on the Illgraben fan is well mixed, probably from multiple episodes of erosion, deposition, and remobilization in sediment reservoirs such as the trunk channel TC1.

Cycles of fill and erosion and of spatial and temporal variability have been documented by previous researchers, e.g., by Bovis and Dagg (1988), Benda (1990), Rickenmann and Zimmermann (1993), Faulkner (1994), Wetzel (1994), Evans and Slaymaker (2004), Schuerch et al. (2006), and Davies and Korup (2007). The concept of channel sediment recharge and subsequent emptying as observed in TC1 (Figs. 5 and 6) is similar to the scenario of sediment availability for debris flow activity (Bovis and Jakob, 1999; Jakob et al., 2005). The Illgraben has been characterized as being more transport-limited than supply-limited (Schlunegger et al., 2009). However, if a channel experiences cycles of fill and scour, sediment availability varies, and sediment supply conditions could vary over time (Faulkner, 1994).

The patterns and particularly the rates of sediment discharge at the Illgraben are exceptional for Alpine standards in that the changes are rapid enough to be documented within an annual and even a seasonal basis. Additionally, as documented by Schlunegger et al. (2009), the large magnitudes of sediment discharge have had an impact on the flow pattern of the receiving trunk stream (i.e., the Rhone River, Fig. 1), and on the overall valley morphology. A crucial question in this context is why erosion and sediment discharge in the Illgraben exceeds the average mean in the Alps by almost two orders of magnitude. As already mentioned by Schlunegger et al. (2009), an answer to these questions requires high-resolution sediment discharge data from other debris flow systems in the Alps, which are currently not available.

5.2. Denudation rates

The bedrock equivalent of sediment transported to the Illgraben outlet by debris flows is 31,500 m^3 for 2008 and 24,000 m^3 for 2009. Corresponding denudation rates for the entire unvegetated catchment area, including the channel zone beneath CD9 and all subcatchments above check dam CD9 (trunk channel TC1 and subcatchments SC2–SC52), are estimated at 13 mm a^{-1} (2008) and 10 mm a^{-1} (2009). We excluded vegetated areas because silt fence measurements in 2006

(Schlunegger et al., 2009) showed that sediment yield from vegetated slopes is two orders of magnitude smaller than from unvegetated slopes. Considering the whole drainage area then would reduce the denudation rates to about 4 mm a^{-1}.

The magnitudes of the denudation rates are consistent with reports of denudation from landslide-dominated hillslopes (Binnie et al., 2007) and from observations of areas characterized by rapid bedrock erosion (DiBiase et al., 2010). Our values are minimum estimates for the catchment because only sediment export by debris flows was included. Estimates from the year 2006 indicate that sediment delivery by floods is <1% of the volume for debris flows (Schlunegger et al., 2009). Thus, debris flow export alone may be sufficient to quantify denudation rates in places where debris flow activity is clearly dominant. Note, however, that this conclusion is based on a short monitoring period and should be confirmed by long-term surveys.

5.3. Debris flow initiation and implications for debris flow entrainment

We observed 11 landslides (nine clearly originating from bedrock) with volumes ranging from 500 to 4400 m^3, but all of these landslides stopped on the hillslope or in the channel below the landslide scar, and none generated debris flows. A reason for the landslides stopping on the hillslope or in the channel could be a reduction in local slope or because the landslides were mostly dry and did not contain enough moisture to fluidize and transform into a debris flow. Because of the large intervals between aerial photographs, it is not possible to precisely determine how these deposits were remobilized. Similar accumulations of landslide-derived sediment in headwater channels that were later entrained and transported out of the system have been previously documented in other mountain ranges (e.g., Benda and Dunne, 1997b; May and Gresswell, 2003; Imaizumi et al. 2006; Brayshaw and Hassan, 2009). It is not possible from these data to determine the exact initiation mechanism of debris flows at the Illgraben.

The observed landslide volumes are several orders of magnitude smaller than the largest observed debris-flow event (about 60,000 m^3 estimated on 1 July 2008 at the outlet into the Rhone River). The volume of sediment eroded from the channel above check dam CD1 (Table 2) is also substantially smaller than the volume of sediment transported out of the catchment by debris flows. This clearly shows that entrainment of sediment stored on the channel bed and banks is essential for the development of a large debris flow, regardless of the initiation mechanism. These observations are corroborated by data on debris flow erosion in the channel on the fan. The magnitudes of measured vertical erosion on the fan are on the order of 1.5 m (between CD28 and CD29) to 4 m (at Bhutan foot bridge; Fig. 7), corresponding to a volume estimate of 26,000 m^3 (2.5 km channel length × 7 m width × 1.5 m erosion). The check dams do not allow net incision; therefore, the channel has to be recharged with sediment between erosive debris-flow events. Deposition in the channel reach on the fan was not studied in detail, but preliminary observations of time-series of photographs of the bed at check dam CD27 suggest that small floods, also during the spring snowmelt, may recharge the channel with sediment. It is also possible that small debris flows may stop in the channel along the fan; however, observations at the Illgraben suggest that this is rare (two such events observed in 10 years). A more precise sediment budget is not possible at this time because of the lack of spatial and temporal data after individual events.

The importance of sediment entrainment and consequent bulking of debris flows has long been acknowledged (Gallino and Pierson, 1984; Benda, 1990; Rickenmann and Zimmermann, 1993; Gabet and Bookter, 2008). In this context, Fannin and Rollerson (1993) showed that debris-flow magnitude was controlled primarily by the volume of material entrained along the channel rather than by the initial landslide volume, yet stressing the importance of debris availability along the channel (Bovis and Jakob, 1999).

6. Summary and conclusions

The Illgraben catchment in Switzerland, one of the most geomorphologically active catchments in the Alps, provides an opportunity to quantify sediment transfer patterns related to debris flow initiation over a yearly timescale. We analyzed aerial image series from fall 2007, summer and fall 2008, and fall 2009 with photogrammetric methods and used them to identify patterns of sediment erosion and deposition. We compared the observed sediment transfer volumes with debris flow magnitudes. The results showed that the debris, often originating from bedrock landslides, was transported in patterns of mobilization, storage, and remobilization, with local storage time <1 year. The trunk channel above the retention dam CD1 was filled during the first half of 2008 by debris from the upslope reaches and was scoured in the second half of 2008, functioning therefore both as reservoir and sediment source. Magnitudes of maximum erosion and deposition decreased from the upper catchment to the Illgraben outlet, but net erosion prevailed over the period of observation. Generally, sediment transfer patterns were variable in space and time and indicated that a high temporal resolution would be needed to document sediment production, subsequent storage, and remobilization, at least in exceptionally active subcatchments. The aerial image frequency we used was insufficient to relate geomorphic change to individual debris flows, and short-term cycles of erosion and deposition may have been missed. Nevertheless, the data are sufficiently detailed to document a successively downslope-directed cascade of sediment transfer mechanisms on a seasonal basis for the smaller-scale tributary systems, and on an annual basis for the Illgraben trunk channel. Additionally, the photogrammetric analysis reveals that landslides with volumes ranging from 500 to 4400 m^3 were observed to stop on the hillslope or in the channel and did not transform directly into debris flows. Landslide volumes are about one order of magnitude smaller than the largest debris flow observed during the study period (debris flow volume estimated at the Illgraben outlet). While it is not possible to dismiss landslide initiation as a viable mechanism of debris flow triggering at the Illgraben, it is clear that debris flows (regardless of the initiation mechanism) must entrain substantial amounts of sediment along the flow path to reach the volumes estimated at the distal end of the fan. Finally, this paper validates the results of previous model-based findings (Benda and Dunne, 1997b; Benda et al., 1998) that sediment transfer in debris flows catchments occurs as sediment pulses on a seasonal and annual basis and thus specifies the temporal scales of sediment discharge.

Acknowledgements

This project was funded by the Competence Center Environment and Sustainability (CCES) of the ETH domain, Switzerland, within the project TRAMM (Triggering of Rapid Mass Movements), and by the Swiss National Science Foundation (project number 200021-119912). We are grateful to the staff of Flotron AG and Perrinjaquet AG for support in the photogrammetry; D. Rieke-Zapp, R. Rosenbauer, P. Thee for help with GPS handling. B. Berger, E. Berger, B. Blum, C. Graf, E. Herzer, F. Iseli, D. Kummer, K. Liechti, M. Pfister, M. Raymond Pralong, B. Nägeli, C. Nydegger, E. Schönthal, R. Sterchi, B. Stricker, H. Vogler assisted during the surveys and field investigations. Y. Bühler, C. Rickli, W.E. Dietrich, and N. Hovius provided helpful comments on an earlier version of the manuscript. We are also grateful for comments from F. Brardinoni and two anonymous reviewers. F. Schlunegger acknowledges support from the ESF TopoEurope project for his involvement in this project.

References

Badoux, A., Graf, C., Rhyner, J., Kuntner, R., McArdell, B.W., 2009. A debris-flow alarm system for the Alpine Illgraben catchment: design and performance. Natural Hazards 49 (3), 517–539. doi:10.1007/s11069-008-9303-x.

Benda, L., 1990. The influence of debris flows on channels and valley floors in the Oregon Coast Range U.S.A. Earth Surface Processes and Landforms 15 (5), 457–466.

Benda, L., Dunne, T., 1997a. Stochastic forcing of sediment routing and storage in channel networks. Water Resources Research 33 (12), 2865–2880.

Benda, L., Dunne, T., 1997b. Stochastic forcing of sediment supply to channel networks from landsliding and debris flow. Water Resources Research 33 (12), 2849–2863.

Benda, L., Miller, D., Dunne, T., Agee, J., Reeves, G., 1998. Dynamic landscape systems. In: Naiman, R., Bilby, R. (Eds.), River Ecology and Management: Lessons from the Pacific Coastal Ecoregion. Springer-Verlag, Reiskirchen, Germany.

Berger, C., 2010. Debris flow entrainment and sediment transfer processes at the Illgraben catchment, Switzerland. Ph.D. thesis, University of Bern, Institute of Geological Sciences, Bern, Switzerland.

Berti, M., Genevois, R., Simoni, A., Tecca, P., 1999. Field observations of a debris flow event in the Dolomites. Geomorphology 29 (3–4), 265–274.

Binnie, S.A., Phillips, W.M., Summerfield, M.A., Fifield, L.K., 2007. Tectonic uplift, threshold hillslopes, and denudation rates in a developing mountain range. Geology 35 (8), 743–746. doi:10.1130/G23641A.1.

Bovis, M.J., Dagg, B.R., 1988. A model for debris accumulation and mobilization in steep mountain streams. Hydrological Sciences - J. des Sciences Hydrologiques 33 (6), 589–604.

Bovis, M., Jakob, M., 1999. The role of debris supply conditions in predicting debris flow activity. Earth Surface Processes and Landforms 24 (11), 1039–1054.

Brardinoni, F., Hassan, M.A., Rollerson, T., Maynard, D., 2009. Colluvial sediment dynamics in mountain drainage basins. Earth and Planetary Science Letters 284, 310–319.

Brayshaw, D., Hassan, M.A., 2009. Debris flow initiation and sediment recharge in gullies. Geomorphology 109 (3–4), 122–131. doi:10.1016/j.geomorph.2009.02.021.

Cannon, S., Reneau, S., 2000. Conditions for generation of fire-related debris flows, Capulin Canyon, New Mexico. Earth Surface Processes and Landforms 25 (10), 1103–1121.

Coe, J.A., Kinner, D.A., Godt, J.W., 2008. Initiation conditions for debris flows generated by runoff at Chalk Cliffs, central Colorado. Geomorphology 96 (3–4), 270–297. doi:10.1016/j.geomorph.2007.03.017.

Davies, T.R.H., Korup, O., 2007. Persistent alluvial fanhead trenching resulting from large, infrequent sediment inputs. Earth Surface Processes and Landforms 32 (5), 725–742. doi:10.1002/esp. 1410.

DiBiase, R.A., Whipple, K.X., Heimsath, A.M., Ouimet, W.B., 2010. Landscape form and millennial erosion rates in the San Gabriel Mountains, CA. Earth and Planetary Science Letters 289, 134–144. doi:10.1016/j.epsl.2009.10.036.

Dietrich, W.E., Dunne, T., 1978. Sediment budget for a small catchment in mountainous terrain. Zeitschrift für Geomorphologie, Supplement Band 29, 191–206.

Dietrich, W.E., Dunne, T., Humphrey, N.F., Reid, L.M., 1982. Construction of sediment budgets for drainage basins. Sediment Budgets and Routing in Forested Drainage Basins: Proceedings of the Symposium; 31 May–1 June 1982, Corvallis, OR. Pacific Northwest Forest and Range Experiment Station, Forest Service, U.S. Department of Agriculture, Washington, DC, pp. 5–23.

Evans, M., Slaymaker, A., 2004. Spatial and temporal variability of sediment delivery from alpine lake basins, Cathedral Provincial Park, southern British Columbia. Geomorphology 61 (1–2), 209–224. doi:10.1016/j.geomorph.2003.12.007.

Fannin, R.J., Rollerson, T.P., 1993. Debris flows: some physical characteristics and behaviour. Canadian Geotechnical Journal 30 (1), 71–81.

Faulkner, H., 1994. Spatial and temporal variation of sediment processes in the alpine semi-arid basin of Alkali Creek, Colorado, USA. Geomorphology 9 (3), 203–222.

Fuller, I.C., Marden, M., 2010. Rapid channel response to variability in sediment supply: cutting and filling of the Tarndale fan, Waipaoa catchment, New Zealand. Marine Geology 270, 45–54. doi:10.1016/j.margeo.2009.10.004.

Gabet, E.J., Bookter, A., 2008. A morphometric analysis of gullies scoured by post-fire progressively bulked debris flows in southwest Montana, USA. Geomorphology 96 (3–4), 298–309. doi:10.1016/j.geomorph.2007.03.016.

Gabus, J.H., Weidmann, M., Bugnon, P.C., Burri, M., Sartori, M., Marthaler, M., 2008. Geological Map of Sierre 1:25,000 (LK 1287, sheet 111). In: Geological Atlas of Switzerland. Swiss Geological Survey, Bern.

Gallino, G.L., Pierson, T.C., 1984. Polallie Creek debris flow and subsequent dam-break flood of 1980, East Fork Hood River Basin, Oregon. Open File-Report 84-578. U.S. Geological Survey, Reston, VA. 37 pp.

Gruber, M., Leberl, F., 2001. Description and evaluation of the high quality photogrammetric scanner UltraScan 5000. ISPRS Journal of Photogrammetry and Remote Sensing 55, 313–329.

Hürlimann, M., Rickenmann, D., Graf, C., 2003. Field and monitoring data of debris-flow events in the Swiss Alps. Canadian Geotechnical Journal 40 (1), 161–175. doi:10.1139/T02-087.

Imaizumi, F., Sidle, R.C., 2007. Linkage of sediment supply and transport processes in Miyagawa Dam catchment, Japan. Journal of Geophysical Research 112, F03012. doi:10.1029/2006JF000495.

Imaizumi, F., Sidle, R.C., Tsuchiya, S., Ohsaka, O., 2006. Hydrogeomorphic processes in a steep debris flow initiation zone. Geophysical Research Letters 33 (10). doi:10.1029/2006GL026250 4 pp.

Iverson, R., Reid, M., LaHusen, R., 1997. Debris-flow mobilization from landslides. Annual Review of Earth and Planetary Sciences 25, 85–138.

Jäckli, H., 1957. Gegenwartsgeologie des bündnerischen Rheingebietes. Ein Beitrag zur exogenen Dynamik alpiner Gebirgslandschaften: Geotechnische Serie 36, Beiträge Geologie Schweiz.

Jakob, M., Hungr, O., 2005. Introduction. In: Jakob, M., Hungr, O. (Eds.), Debris-flow Hazards and Related Phenomena. Springer, Berlin, pp. 1–8.

Jakob, M., Bovis, M., Oden, M., 2005. The significance of channel recharge rates for estimating debris-flow magnitude and frequency. Earth Surface Processes and Landforms 30, 755–766. doi:10.1002/esp. 1188.

Larsen, I.J., Pederson, J.L., Schmidt, J.C., 2006. Geologic versus wildfire controls on hillslope processes and debris flow initiation in the Green River canyons of Dinosaur National Monument. Geomorphology 81 (1–2), 114–127. doi:10.1016/j.geomorph.2006.04.002.

Lichtenhahn, C., 1971. Zwei Betonmauern: Die Geschieberückhaltesperre am Illgraben (Wallis) und die Staumauer des Hochwasserschutzbeckens an der Orlegna im Bergell (Graubünden). International Symposium Interpraevent. F.f.v. Hochwasserbekämpfung 3, 451–456.

Major, J.J., Pierson, T.C., Scott, K.M., 2005. Debris flows at Mount St. Helens, Washington, USA. In: Jakob, M., Hungr, O. (Eds.), Debris-flow Hazards and Related Phenomena. Springer, Berlin, pp. 685–731.

May, C., Gresswell, R., 2003. Processes and rates of sediment and wood accumulation in headwater streams of the Oregon Coast Range, USA. Earth Surface Processes and Landforms 28 (4), 409–424.

McArdell, B.W., Graf, C., 2009. Field observations of debris flow properties at the Illgraben catchment, Switzerland. Geological Society of America Annual Meeting 2009. Paper No. 240-3.

McArdell, B.W., Bartelt, P., Kowalski, J., 2007. Field observations of basal forces and fluid pore pressure in a debris flow. Geophysical Research Letters 34 (7). doi:10.1029/2006GL029183 4 pp.

Rickenmann, D., Zimmermann, M., 1993. The 1987 debris flows in Switzerland—documentation and analysis. Geomorphology 8 (2–3), 175–189.

Rickenmann, D., Hürlimann, M., Graf, C., Näf, D., Weber, D., 2001. Murgang-Beobachtungsstationen in der Schweiz. Wasser Energie Luft 93 (1/2), 1–8.

Santi, P.M., deWolfe, V.G., Higgins, J.D., Cannon, S.H., Gartner, J.E., 2008. Sources of debris flow material in burned areas. Geomorphology 96 (3–4), 310–321. doi:10.1016/j.geomorph.2007.02.022.

Schlunegger, F., Badoux, A., McArdell, B.W., Gwerder, C., Schnydrig, D., Rieke-Zapp, D., Molnar, P., 2009. Limits of sediment transfer in an alpine debris-flow catchment, Illgraben, Switzerland. Quaternary Science Reviews 28, 1097–1105. doi:10.1016/j.quascirev.2008.10.025 (11–12, Sp. Iss. SI).

Schrott, L., Hufschmidt, G., Hankammer, M., Hofmann, T., Dikau, R., 2003. Spatial distribution of sediment storage types and quantification of valley fill deposits in an alpine basin, Reintal, Bavarian Alps, Germany. Geomorphology 55 (1–4), 45–63. doi:10.1016/S0169-555X(03)00131-4.

Schuerch, P., Densmore, A.L., McArdell, B.W., Molnar, P., 2006. The influence of landsliding on sediment supply and channel change in a steep mountain catchment. Geomorphology 78 (3–4), 222–235. doi:10.1016/j.geomorph.2006.01.025.

Schumm, S.A., 1977. The Fluvial System. Wiley, New York.

Slaymaker, O., Souch, C., Menounos, B., Filippelli, G., 2003. Advances in Holocene mountain geomorphology inspired by sediment budget methodology. Geomorphology 55 (1–4), 305–316. doi:10.1016/S0169-555X(03)00146-6.

Stock, J.D., Dietrich, W.E., 2006. Erosion of steepland valleys by debris flows. Geological Society of America Bulletin 118 (9–10), 1125–1148. doi:10.1130/B25902.1.

Wetzel, K.F., 1994. The significance of fluvial erosion, channel storage and gravitational processes in sediment production in a small mountainous catchment area. In: Ergenzinger, P., Schmidt, K.H. (Eds.), Dynamics and Geomorphology of Mountain Rivers. Springer, Berlin.

Wieczorek, G.F., 1987. Effect of rainfall intensity and duration on debris flows in central Santa Cruz Mountains, California. Geological Society of America Reviews in Engineering Geology 7, 93–104.

Zimmermann, M., Mani, P., Romang, H., 1997. Magnitude–frequency aspects of alpine debris flows. Eclogae geologicae Helvetiae 90 (3), 415–420.